Wireless and mobile systems course project: Indoor passive localization system based on the CSI

Zhaowei Zhu, Student ID:14520873
Hanyu Zhu, Student ID:89873352

January 12, 2018

1 System Architecture

In this report, we propose a novel indoor passive positioning system based on the existing commercial WiFi system. The signal we use is the 2.4GHz WiFi signal following the 802.11n protocol. The transmitter is a general access point (AP) and the receiver is a personal computer. Using this system, we can locate a person when the target is free of any positioning equipments. Fig. 1

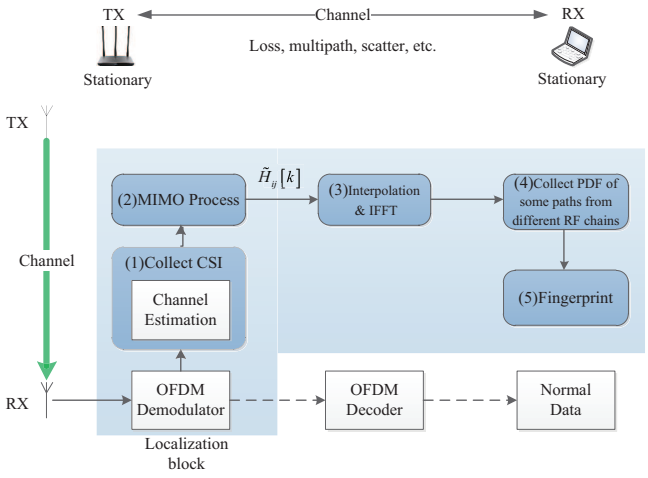

Figure 1: System architecture

illustrates the system architecture of our localization system. The WiFi signal following the 802.11n protocol is sent from one stationary transmitter to a stationary personal computer, received by a network interface card (NIC). The blocks in light color such as the OFDM demodulator are processes handled by the NIC. Our system is built on an existing WiFi communication system and the CSI is provided by a commercial NIC named Intel5300. The processing scheme mainly includes 5 parts as Fig. 1.

Firstly, if there are any packets following 802.11n protocol between TX (the AP) and RX (the personal computer), the CSI of each packet is given and recorded after channel estimation in the physical layer. According to the 802.11n protocol, each packet can provided CSI from 30 different subcarriers. After that, these 30 subcarriers are obtained in the frequency domain. In order to combine this information with multi-path effect, linear interpolation and 64-point fast Fourier fransform(FFT) are carried out for these 30 subcarriers so as to get one 64-point sequence in time domain, which is the reflection of multi-path effect. Then the probability distribution functions

(PDF) of some path amplitudes are calculated for fingerprint, severing as the training data or the testing data. Finally, the most possible area is selected by performing the maximum likelihood (ML) method.

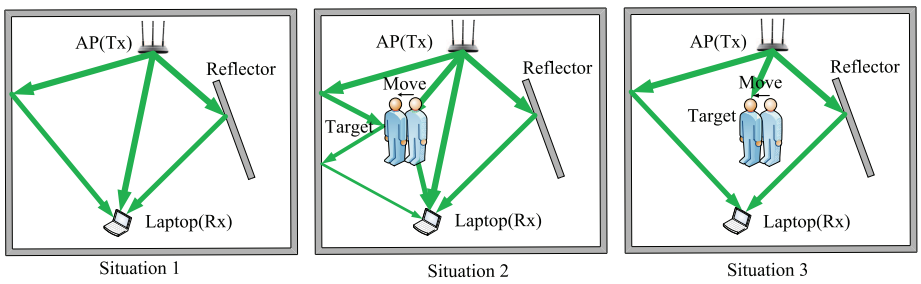

Figure 2: People's influence on channel state

Fig. 2 describes three typical situations for people's influence on indoor environment. When someone is walking in the monitor area, it is indispensable to obstruct or reflect some paths more or less [1].

The proposed system is built on the CSI-tool [2] which is jointly built by University of Washington, Microsoft Research Asia and Intel Labs Seattle jointly. It runs on a commodity 802.11n NIC, Intel WiFi Link 5300 wireless NIC. And it works well on Linux operating system Ubuntu 10.04 LTS with the 2.6.36 kernel and some newer Linux releases.

2 MIMO Signal Model

Consider the multipath situation, channel between the transmitting antenna i and receiving antenna j can be written as $\widetilde{H}_{ij}[k]$,

$$\widetilde{H}_{ij}[k] = H_f[k] \exp\left[j\left(\theta_{ij} - 2\pi k \frac{n_{0,ij}}{N}\right)\right] \sum_{m_{ij}=0}^{M_{ij}-1} \alpha_{m_{ij}} \exp\left(-j2\pi k \frac{n_{m_{ij}}}{N}\right). \tag{1}$$

For one packet provided by a single NIC, θ_{ij} and $n_{0,ij}$ are the same respectively since there is only one reference clock. Therefore, $\widetilde{H}_{ij}[k]$ is simplified as

$$\widetilde{H}_{ij}[k] = H_f[k] \exp(j\theta) \exp\left(-j2\pi k \frac{n_0}{N}\right) \Phi_{k,ij}, \tag{2}$$

where $\theta \sim U(-\pi, \pi)$ is the phase offset caused by the carrier frequency offset (CFO), $n_0 \sim U(-1/2, 1/2)$ is the sampling time offset [3, 4], and

$$\Phi_{k,ij} = \sum_{m_{ij}=0}^{M_{ij}-1} \alpha_{m_{ij}} \exp\left(-j2\pi k \frac{n_{m_{ij}}}{N}\right) = \alpha_{k,ij} \exp\left(-j2\pi k \frac{n_{ij}}{N}\right). \tag{3}$$

Note the variables θ and n_0 of different paths can be canceled out by each other since they are the same in one packet. In other words, if $\widetilde{H}_{11}[k]$ is selected as reference, i.e, let

$$\begin{aligned} \hat{H}_{ij}[k] &= \frac{\widetilde{H}_{ij}[k]}{\widetilde{H}_{11}[k]} \left|\widetilde{H}_{11}[k]\right| = \alpha_{k,11} |H_f[k]| \frac{\Phi_{k,ij}}{\Phi_{k,11}} = |H_f[k]| \frac{\sum_{m_{ij}=0}^{M_{ij}-1} \alpha_{m_{ij}} \exp\left(-j2\pi k \frac{n_{m_{ij}}}{N}\right)}{\exp\left(-j2\pi k \frac{n_{11}}{N}\right)} \\ &= |H_f[k]| \sum_{m_{ij}=0}^{M_{ij}-1} \alpha_{m_{ij}} \exp\left(-j2\pi k \frac{n_{m_{ij}} - n_{11}}{N}\right). \end{aligned} \tag{4}$$

Hence $\hat{H}_{ij}[k]$ can be regarded as relative multipath effects in the frequency domain. By performing IDFT on $\hat{H}_{ij}[k]$, the multipath effects in the time domain is obtained as

$$\hat{h}_{ij}[n] = \frac{1}{N}\sum_{k=0}^{N-1}\hat{H}_{ij}[k]\exp\left(j2\pi k\frac{n}{N}\right) = \sum_{m_{ij}=0}^{M_{ij}-1}\alpha_{m_{ij}}h\left[n-n_{m_{ij}}+n_{11}\right], \tag{5}$$

where M_{ij} is the possible total number of paths between the transmitter i and the receiver j, and

$$h[n] \triangleq \frac{1}{N}\sum_{k=0}^{N-1}|H_f[k]|\exp\left(j2\pi k\frac{n}{N}\right). \tag{6}$$

In this way, a expression for multipath effect in the time domain is derived.

3 Preprocessing algorithm

In this section, the proposed model will be reviewed briefly and the pseudo-code for the preprocessing procedure will be given.

Algorithm 1 Preprocessing

Function Preprocessing$\tilde{\mathbf{H}}$
for all $i, j = 1, 2, k = 1, 2, ..., 30$ **do**
  $\hat{H}_{ij}[k] \leftarrow \frac{\tilde{H}_{ij}[k]}{\tilde{H}_{11}[k]}\left|\tilde{H}_{11}[k]\right|$
end for
Delete $\hat{\mathbf{H}}_{11}$ from $\hat{\mathbf{H}}_{ij}$, the rest form $\hat{\mathbf{H}}_i, i = 1, 2, 3$
for all $i = 1, 2, 3$ **do**
  $\hat{\mathbf{H}}_i \leftarrow$ **Interpolation**$(\hat{\mathbf{H}}_i)$
  $\hat{\mathbf{h}}_i \leftarrow$ **IFFT**$(\hat{\mathbf{H}}_i)$
end for
return $\hat{\mathbf{h}}$
EndFunction

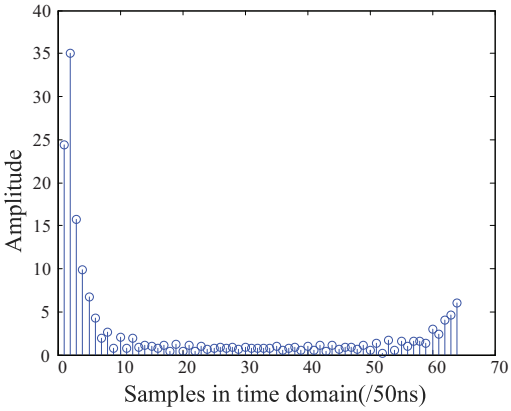

Figure 3: CSI in the time domain

We finally obtain the relative multipath effect referring to a certain RF chain, e.g., the RF chain between the 1-st transmitter and the 1-st receiver. In order to make the physical meaning more clear, the inverse Fourier transform is carried out for the interpolated CSI and the relative multipath effect in the time domain is derived. Consider a 2×2 MIMO system, the pseudo-code of this procedure is listed as **Algorithm 1**.

In this algorithm, the reference CSI in the frequency domain, i.e. $\hat{\mathbf{H}}_{11}$, is deleted because it has less information than the others, i.e., only amplitude information in the reference RF chain is derived according to (4). For the output of this algorithm, let

$$\hat{\mathbf{h}} = [\hat{\mathbf{h}}_1, \hat{\mathbf{h}}_2, \hat{\mathbf{h}}_3], \tag{7}$$

where $\hat{\mathbf{h}}_i, i = 1, 2, 3$ is a 64-point column vector on behalf of 64 samples in the time domain, i.e., the first point in this vector represents the first sampled path.

4 Experiments and Results

4.1 Experiments

In this section, we explain the experimental procedures and show the performance of our localization system. In order to evaluate the performance, an experiment is conducted at a $11m \times 7m$ office

in ShanghaiTech University. The AP to transmit the WiFi signal is a type of commercial wireless router made by the Mercury company. The receiver is a Dell personal computer equipped with the network interface card Intel5300, which is driven by the CSI-tool in Ubuntu. CSI is collected using this tool. During the experiment, the personal computer connects to the WiFi generated by the AP and uses *ping* to communicate with the connected AP so as to get a stable collecting rate, which is 20Hz in the experiment. Two antennas in the transmitter and two in the receiver constitute a MIMO system based on the 802.11n protocol. The frequency and bandwidth of which are 2.4GHz and 20MHz respectively. Experimental procedures mainly contain the training phase and the testing phase as follows.

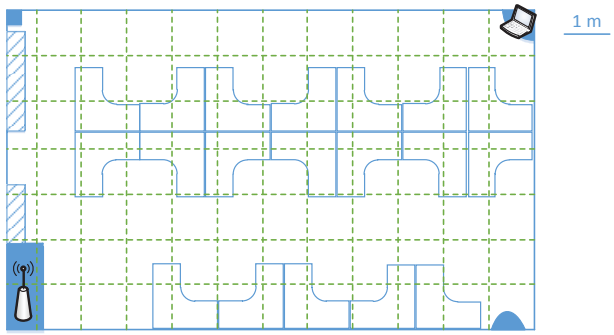

Figure 4: Experimental environment

4.1.1 Training phase

At the training phase, the classroom is divided into 77 grids, based on 7 rows between the AP and the personal computer as is shown in Fig. 4. Each row is uniformly divided to 11 grids. To ensure the fairness of data from each area, someone was walking slowly from one side of a row to another side. The fairness refers to the same amount of CSI in each location.

In the meanwhile, the CSI is collected and recorded through the CSI-tool. Data collected from each row is separated into 11 parts uniformly which is corresponding to 11 grids in this row. Then the CSI is processed according to Fig. 1 till stage 4. Using this collecting method, accurate fingerprints can be easily obtained for each grid.

Denote the training PDF for a certain grid by $\mathbf{Q}$ and $\mathbf{Q} = \{\mathbf{Q}_{ij}\}$, where i represents the i-th RF chain and j is the j-th path. In the training phase, we first gather enough CSI at each grid. Then the *Preprocessing* is performed for each grid to get the CSI in the time domain. The algorithm is listed in **Algorithm 2**.

Algorithm 2 Training Phase

Function Training$\widetilde{\mathbf{H}}^{(k)}, k = 1, 2, 3, ..., K$
  for all $k = 1, 2, 3, ..., K$ **do**
    $\hat{\mathbf{h}}^{(k)} \leftarrow$ **Preprocessing** $\left(\widetilde{\mathbf{H}}^{(k)}\right)$
  end for
  for all $i = 1, 2, 3, j = 1, 2, 3, ..., T_j$ **do**
    $\mathbf{Q}_{ij} \leftarrow \underset{k=1,2,...,K}{\text{PDF}} \left(\left|\hat{h}_{ij}^{(k)}\right|\right)$
  end for
  $\mathbf{Q} \leftarrow \{\mathbf{Q}_{ij}\}$
  return $\mathbf{Q}$
  EndFunction

Algorithm 3 Testing Phase

Function Testing$\widetilde{\mathbf{H}}^{(k)}, k = 1, 2, 3, ..., K$
  for all $k = 1, 2, 3, ..., K$ **do**
    $\hat{\mathbf{h}}^{(k)} \leftarrow$ **Preprocessing** $\left(\widetilde{\mathbf{H}}^{(k)}\right)$
  end for
  for all $i = 1, 2, 3, j = 1, 2, 3, ..., T_j$ **do**
    $\mathbf{P}_{ij} \leftarrow \underset{k=1,2,...,K}{\text{PDF}} \left(\left|\hat{h}_{ij}^{(k)}\right|\right)$
  end for
  $\mathbf{P} \leftarrow \{\mathbf{P}_{ij}\}$
  for all $r = 1, 2, 3, ..., R$ **do**
    Match $\mathbf{P}$ with the training PDF $\mathbf{Q}_r$ using (8)
  end for
  Get the most possible grid μ according to (9)
  return μ
  EndFunction

The inputs $\widetilde{\mathbf{H}}^{(k)}, k = 1, 2, 3, ..., K$ of this algorithm are the CSI in a grid. K is the number of observations. $\mathbf{H}^{(k)}$ is the k-th observation. In this algorithm, PDFs for the CSI in T_j paths and all RF chains are obtained. T_j is the threshold of useful paths, as is indicated in Fig. 3. $T_j = 3$ in the actual algorithm. In other words, under the experimental settings that there are three useful RF chains and three useful paths each RF chain, the number of PDFs for each grid is $3 \times 3 = 9$, i.e., there are 9 elements in $\mathbf{Q}$.

4.1.2 Testing phase

In the testing phase, a person walks, turns around and does other irregular motions in the detection area. The CSI is collected for each grid as is allocated in the training phase. In order to obtain a probability distribution, a window is set to select a group of CSI data. For example, the window length is 200, which amounts to the number of CSI packets collected in one second. It slides forward several packets every time, so as to choose another group of data. Suppose that there are 2000 packets collected in one region, then 1801 groups will be created.

After obtaining the testing probability distribution, the next step is finding the most possible region using ML method. Assuming that the testing PDF is $\mathbf{P} = \{\mathbf{P}_{ij}\}$, where i, j represent the i-th RF chain and the j-th path. We assume all RF chains and paths are statistically independent. Thus the probability of the i-th RF chain matching with the r-th region $p_{i,r}$ is $p_{i,r} \propto \prod_{j=1}^{3} p_{ij,r}$ where $p_{ij,r} \propto \frac{1}{D_{JS}(\mathbf{P}_{ij} \| \mathbf{Q}_{ij,r})}$. The joint probability of three RF chains towards the r-th region is $p_r \propto \prod_{i=1}^{3} p_{i,r}$. Then we can obtain

$$\ln p_r = -\sum_{i=1}^{3}\sum_{j=1}^{3} D_{JS}\left(P_{ij} \| Q_{ij,r}\right) + C, \tag{8}$$

where C is a constant and stays the same for one test group. The most possible region is

$$\mu = \arg\max_r p_r = \arg\max_r \ln p_r. \tag{9}$$

The algorithm of the testing phase is given as **Algorithm 3**. The preprocessing part is similar to that in the **Algorithm 2**.

4.2 Result and discussion

In this section, we will discuss some traits of the channel state information in the time domain and analyze the localization performance of different methods. Firstly, we will show that the CSI is more clear after the proposed MIMO process. Fig. 5 shows a comparison about the CSI amplitude in the first path of the time domain without and with the MIMO process algorithm. The upper one shows the changing of CSI amplitude in the time domain when one person walks in one-meter area. The fluctuation of this wave is fierce. Plenty of noises cover the real signal due to the time offset. It is nearly original data because we only do interpolation and IFFT on the raw data from the NIC. Considering the time offset and other effects, MIMO process are performed on the raw data in order to eliminate the noise as much as possible, the result of which is given in the subplot two in Fig. 5. It is obviously that most noises are canceled and the signal is clearer than before. Thus the *Preprocessing* algorithm works.

4.2.1 CSI characteristics in the time domain

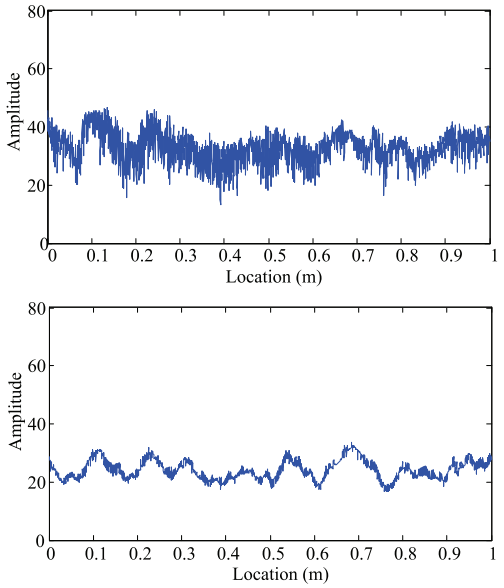

Figure 5: CSI amplitude without and with MIMO Process

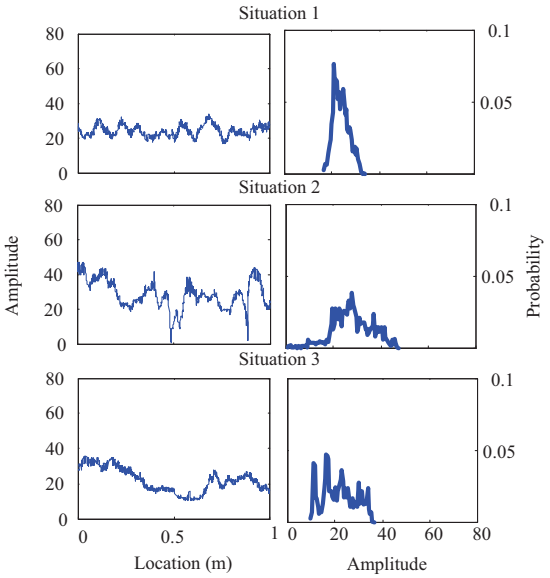

Figure 6: CSI in different location

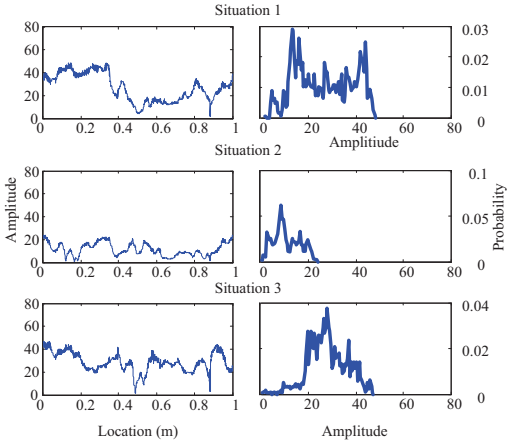

Figure 7: CSI in different RF chains

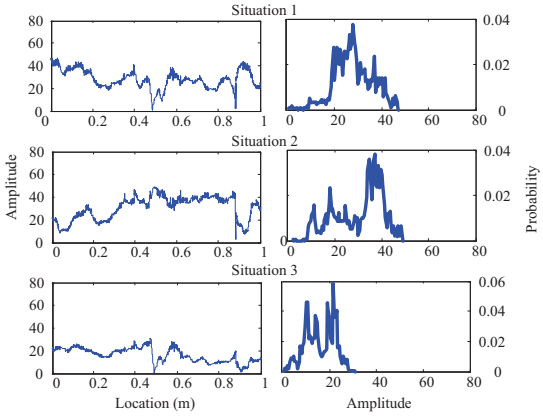

Figure 8: CSI in different paths

The CSI amplitude is different versus people's locations, no matter in the frequency domain or time domain. According to the procedure in function *Preprocessing*, the specific CSI in the time domain is obtained. Fig. 6 shows the CSI amplitude and its PDF in three different situations, each of which belongs to different areas. The selected amplitude changes evidently with locations. What's more, the overall levels and sensitivities are different from each other. Fig. 6 also reveals that the amplitude distribution is different when people walking in different areas. Let the amplitude distribution to be a dependent variable, thus the detection area is an independent variable.

4.2.2 Localization precision using different PDF difference metrics

Fig. 9 shows the localization performance under the circumstance of a classroom in Fig. 4. The detection area is the whole classroom which is divided into 77 parts. Three lines in Fig. 9 represent the Cumulative Distribution Function(CDF) of the distance error using the JS divergence, KL

divergence and EMD, respectively. The JS divergence metric has the best performance in Mean Absolute Difference(MAD) which is 2.48m, while the KL divergence metric is 1m worse in MAD than the JS divergence. It may be on account of the asymmetrical form in the KL divergence, which is not robust enough. The EMD metric has similar performance to the JS divergence, only a little worse.

The result of this experiment shows that the JS divergence works better than the EMD. And it is obviously that the JS divergence is an effective method with lower complexity than the EMD. As a consequence, the JS divergence metric is finally chosen as the measure the PDF distances.

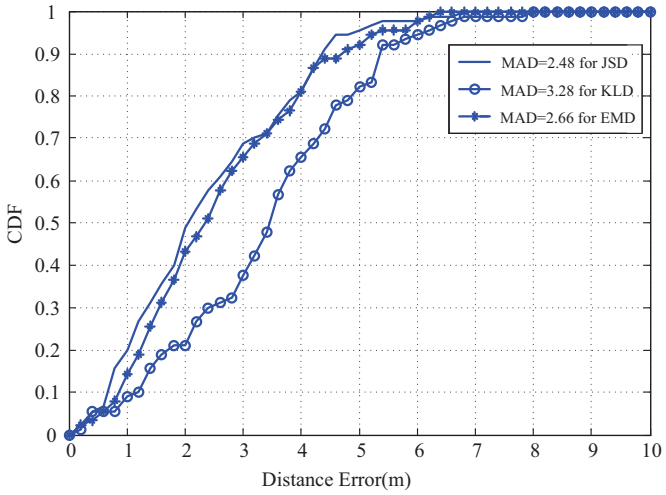

Figure 9: Performance of three PDF difference metrics

5 Conclusion and Future Work

In this report, we've designed and implemented a WiFi-based sensing system for passive localization. We've analyzed the CSI model in detail, and put forward a MIMO processing algorithm. Then we've verified the proposed method with some experiments. There are still lots of works to do. From the signal aspect, how to use make better use of CSI given by the NIC, how to repeat these experiments in the USRP and how to get more information using the USRP are tough problems to be solved. From the system aspect, how to improve the system from a single-transmitter signal-receiver one to a multi-transmitter multi-receiver one is still a problem. What's more, we should explore how to combine the passive localization result with the active localization result. Besides, the multi-target situation is also tough to figure out.

References

[1] Y. Wang, K. Wu, and L. M. Ni, "WiFall: Device-Free Fall Detection by Wireless Networks," *IEEE Trans. Mobile Comput.*, vol. 16, no. 2, pp. 581–594, Feb. 2017.

[2] D. Halperin, W. Hu, A. Sheth, and D. Wetherall, "Tool release: gathering 802.11 n traces with channel state information," *ACM SIGCOMM Comput. Commun. Review,* vol. 41, no. 1, pp. 53-53, 2011.

[3] K. Qian, C. Wu, Z. Yang, Y. Liu and Z. Zhou, "PADS: Passive detection of moving targets with dynamic speed using PHY layer information," in *P*roc. IEEE ICPADS, Hsinchu, Dec. 2014, pp. 1–8.

[4] C. Wu, Z. Yang, Z. Zhou, K. Qian, Y. Liu and M. Liu, "PhaseU: Real-time LOS identification with WiFi," in *P*roc. IEEE INFOCOM, Kowloon, Aug. 2015, pp. 2038–2046.